Isotopic 18O/16O Substitution Study on the Direct Partial Oxidation of CH4 to Dimethyl Ether over a Pt/Y2O3 Catalyst Using NO/O2 as an Oxidant

Journal:	*Catalysis Science & Technology*
Manuscript ID	CY-COM-02-2021-000253.R1
Article Type:	Communication
Date Submitted by the Author:	13-Mar-2021
Complete List of Authors:	Ghampson, Isaac Tyrone; Tokyo Metropolitan University - Minamiosawa Campus, Applied Chemistry for Environment Lundin, Sean-Thomas; The University of Tokyo Shishido, Tetsuya; Tokyo Metropolitan University, Applied Chemistry for Environment Oyama, S.; Virginia Polytechnic Institute and State University, Chemical Engineering

COMMUNICATION

Isotopic $^{18}O/^{16}O$ Substitution Study on the Direct Partial Oxidation of CH_4 to Dimethyl Ether over a Pt/Y_2O_3 Catalyst Using NO/O_2 as an Oxidant

Received 00th January 20xx,
Accepted 00th January 20xx

DOI: 10.1039/x0xx00000x

I. Tyrone Ghampson,[b,c] Sean-Thomas B. Lundin,[c] Tetsuya Shishido [b] and S. Ted Oyama *[a,c,d]

The direct partial oxidation of CH_4 to dimethyl ether (DME) was achieved with a Pt/Y_2O_3 catalyst using a mixture of NO and O_2. The actual gas composition contained a mixture of NO and NO_2, with no decomposition or net consumption of these species. Use of $^{18}O_2$ confirmed the transfer of labeled oxygen from O_2 to CH_4, indicating the NO/NO_2 mixture worked as a single oxygen atom shuttle.

The direct partial oxidation of methane to transportable liquid oxygenate products is highly desirable as many natural gas reserves are found in remote locations. The subject has been studied extensively and is covered in a number of recent reviews.[1-5] So far, only moderate progress has been made because methane is unreactive and harsh conditions are needed for its activation. In a recent study, the direct oxidation of methane to dimethyl ether (DME) at mild conditions was demonstrated for the first time using a Pt/Y_2O_3 catalyst and a mixture of NO and O_2.[6] The reaction did not form N_2, indicating that NO and NO_2 were cycling and O_2 was the ultimate oxidant. Contact time analysis showed that DME was formed directly without formation of methanol – an unprecedented finding that was linked to a surface reaction between adsorbed methyl and methoxide groups formed from nitrate species on the catalyst. Here, O_2 is confirmed to be the terminal oxidant by isotopic labeling.

Prior work described in the aforementioned reviews employed a multitude of catalysts and a variety of oxidizing agents but produced unsatisfactory results. Oxidation with molecular oxygen generally requires high temperatures because of the low reactivity of methane, but this results in uncontrolled oxidation of the desired products. To overcome this problem activated oxidants such as H_2O_2[7,8] and N_2O[9, 10] have been used to lower reaction temperatures and reduce overoxidation. These oxidants are more active and selective than O_2, but are expensive and decompose during the reaction. Therefore, it is preferable to functionalize methane using O_2 directly, even if a separation step for an assistive oxidant is required. A similar situation exists with propylene oxidation.[11] In the previous work[6] with NO and O_2 the specific origin of the oxygen was not directly substantiated. The present work utilizes isotopically labeled oxygen $^{18}O_2$ to demonstrate the formation of ^{18}O-labeled DME and elucidate the mechanism.

Isotopic experiments have been used effectively in mechanistic studies.[12, 13] For example, in oxidation reactions isotopic oxygen ($^{18}O_2$) has been utilized to give information about the type of mechanism (Mars-van Krevelen or Langmuir-Hinshelwood) by exchange of gas-phase O_2 with lattice oxygen[14-16] and the identity of adsorbed intermediates by shifts in vibrational frequency.[16, 17] In a seminal study, Keulks used $^{18}O_2$ to demonstrate the participation of lattice oxygen in the catalytic oxidation of propylene to acrolein on bismuth molybdate by showing that only a small fraction of the oxygen in the products was labeled.[18] Many subsequent studies on both partial oxidation[19] and complete combustion[20] with $^{18}O_2$ have confirmed the involvement of lattice oxygen, whereas only a few have shown the participation of adsorbed oxygen.[14] The previous studies were useful in providing evidence for the type of oxygen involved in catalytic oxidation but gave little to no information on the kinetic isotope effect for $^{18}O/^{16}O$ because the difference in their reactivity was small. In this paper, a kinetic isotope effect is estimated.

The preparation of the Pt/Y_2O_3 catalyst and calculation of dispersion and particle size are in the Electronic Supplementary Information (ESI). In brief, the sample (2 wt% Pt loading) was prepared by incipient wetness impregnation of $H_2PtCl_6{\cdot}6H_2O$ on a commercial Y_2O_3 support and was reduced at 400 °C prior to use. Yttria was chosen because among various supports tested (e.g. SiO_2, CeO_2, TiO_2, and $CaCO_3$), it was shown to be effective in producing DME.[21] The surface area and chemisorption properties of the catalyst are summarized in Table 1.

[a] School of Chemical Engineering, Fuzhou University, Fuzhou 350116, China. E-mail: oyama@vt.edu
[b] Department of Applied Chemistry for Environment, Graduate School of Urban Environmental Sciences, Tokyo Metropolitan University, 1-1 Minami-Osawa, Hachioji, Tokyo 192-0397, Japan.
[c] Department of Chemical System Engineering, The University of Tokyo, 7-3-1 Hongo, Bunkyo-ku, Tokyo 113-8656, Japan.
[d] Department of Chemical Engineering, Virginia Tech, Blacksburg, VA 24061, United States.
Electronic Supplementary Information (ESI) available. See DOI: 10.1039/x0xx00000x

Table 1. Physical characteristics of the Pt/Y_2O_3 catalyst

Catalyst	Surface area / $m^2\ g^{-1}$	CO uptake / $\mu mol\ g^{-1}$	Dispersion (%)	Particle size/ nm
Pt/Y_2O_3	96	98	94	1.2

Steady-state reactivity results are reported in detail elsewhere[6] and will only be discussed briefly here. Methane conversion ranged from 0.03% to 1.5% and DME selectivity was between 2% and 44%. DME was formed only when NO and O_2 were used in combination as the oxidant, whereas only CO_2 was produced when O_2 was used alone (Fig. S1). The maximum DME formation rate was 26 $\mu mol\ g^{-1}\ h^{-1}$, which is comparable to the best catalytic oxygenate productivities reported with activated oxidants such as N_2O[9, 10] and H_2O_2.[7] As a reference to the Pt/Y_2O_3 catalyst, similar measurements were made for a Pt/SiO_2 catalyst and CO_2 was the only carbon-containing product observed. The reactivity behavior of Pt/Y_2O_3 is attributed to partially oxidized Pt sites observed by in situ X-ray absorption spectroscopy[6] formed by interaction with the Y_2O_3 support and the high dispersion (Table 1). It is possible that Pt coexists in oxidized and reduced states as shown for CO oxidation on Pt/Ceria.[22] Here the Pt likely cycles in oxidation state as species like bridging nitrate species (Fig. 3), observed by in situ infrared spectroscopy[21], form and react in the catalytic cycle.

The oxidation of NO to NO_2 occurs readily in the gas phase either through the formation of NO dimers or NO_3 intermediates (ESI, eqns. 3-7).[23] The specific steps involved are consequential here only as they relate to the formation of surface nitrate species. In that regard, previous in situ FTIR measurements gave evidence of the involvement of NO_3 but not $(NO)_2$ species.[6] The facile oxidation reaction is demonstrated by a video in the ESI, which shows that colourless NO gas transforms rapidly into dark brown NO_2 even at room temperature. Thermodynamic calculations (Fig. S3) show that NO and NO_2 coexist in substantial amounts between 250 °C and 400 °C, which is the temperature range of interest in methane partial oxidation catalysis. This indicates that NO and NO_2 are cycling and can potentially deliver single atomic oxygen equivalents (Fig. S2). Past work indicated that the single oxygen atom was derived from molecular oxygen.[6] In this work isotope substitution experiments were conducted to verify that oxygen from O_2 was transferred to methane via the NO/NO_2 shuttle.

Isotopic substitution of oxygen was carried out at the temperature where the maximum DME formation rate was obtained (325 °C). Initially, the reduced catalyst was exposed to the reactant gas mixture until steady-state conditions were achieved, and then the flow of $^{16}O_2$ was replaced by He. Mass signals corresponding to all potential gaseous reactants and products were monitored but only the most relevant masses are shown here for brevity. The figures to be presented are divided into two panels in which the top presents MS signals of the reactants (m/z = 16, 30, 32 and 36) and the bottom presents MS signals of the products (m/z = 44, 45, 46 and 47). Ignoring peaks contributing less than 7%, the expected fragmentation pattern contributions (from NIST Webbook) for all potential reactants and products are shown in Fig. S4. The mass signals shown are 16 (CH_4), 30 ($N^{16}O$, $N^{16}O_2$ and $N^{16}O^{18}O$), 32 ($^{16}O_2$ and $N^{16}O^{18}O$), 36 ($^{18}O_2$), 44 ($C^{16}O_2$), 45 ($CH_3{}^{16}OCH_3$), 46 ($CH_3{}^{16}OCH_3$, $N^{16}O_2$ and $C^{16}O^{18}O$) and 47 ($CH_3{}^{18}OCH_3$).

Fig. 1 shows the transitions from steady-state reaction in $^{16}O_2$ (left), reaction without $^{16}O_2$ (middle), and pulsing with $^{16}O_2$ (right). After $^{16}O_2$ had been switched off, the $C^{16}O_2$ and $CH_3{}^{16}OCH_3$ signals fell to their respective baselines within ca. 2 min. This rapid decline is attributed to depletion of $^{16}O_2$ and is consistent with the negligible CH_4 reactivity with NO alone as the oxidant from steady-state measurements.[6] The results also indicate that oxygen from the Y_2O_3 support and electron deficient Pt sites did not significantly contribute to the reaction, confirming that molecular oxygen in the gas phase is indispensable for the formation of DME.

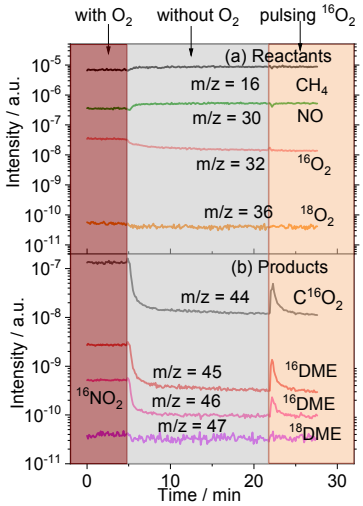

Fig. 1. MS signals versus time showing truncated region of an initial stabilization step with the reactant gas mixture (CH_4:NO:O_2:inert = 20:1:1:78), a subsequent step with the O_2 flow switched off (CH_4:NO:inert = 20:1:78), and the first pulse from the $^{16}O_2$ pulsing step. Conditions: 100 mg of catalyst, 325 °C, 0.1 MPa.

Fig. 2 shows the results of the isotope labeling pulse measurements. Pulsing began after the initial stabilization period showed no appreciable changes in the mass signals over time. The results are organized into three sections in the order of the sequence of measurements: (1) pulsing $^{16}O_2$, (2) pulsing $^{18}O_2$ after flushing with He, and (3) pulsing $^{16}O_2$ after flushing with He to verify the catalyst performance had not changed.

For all three sections of the experiment, the mass 16 (CH_4) signal (Fig. 2a, c and e) is featureless due to the low reactivity of methane; conversion is estimated from the products to be ca. 0.025%. The mass 30 ($N^{16}O$) signal shows dips with each oxygen pulse because some $N^{16}O$ is consumed to form NO_2.

The first section shows results of pulsing with $^{16}O_2$, and the mass 32 signal (Fig. 2a) is likely associated with unreacted $^{16}O_2$. The pulses appear low because the gain for that mass was set to a low value, but the peaks can be discerned. The observed product peaks (Fig. 2b) correspond to the expected carbon-containing compounds from pulsing $^{16}O_2$, namely, $C^{16}O_2$ (m/z = 44) and $CH_3{}^{16}OCH_3$ (m/z = 45 and 46). As shown, the signals of the products dropped to the baselines within 3 min as the

concentration of the reactant stream was depleted of $^{16}O_2$. This is consistent with the earlier determination that molecular oxygen in the gas phase is key to this reaction. Integration of the areas for the m/z = 44 and m/z = 45 peaks and comparison to areas from calibrated pulses of the corresponding gases gave the amount of $C^{16}O_2$ produced to be 12 ± 1 μmol g^{-1} and that of $CH_3{}^{16}OCH_3$ formed to be 0.62 ± 0.06 μmol g^{-1}.

The second section shows the results of pulsing $^{18}O_2$ (Fig. 2c and d). Although not shown, there was no mass 34 signal change due to $^{16}O^{18}O$ formation, suggesting $^{16}O_2$ was completely purged by flowing pure He and the O_2 consumption reactions were not reversible. This result also suggests that isotopic exchange over Y_2O_3 did not occur. This could be due to the lower reaction temperature used since it has been reported that hetero-exchange reaction between a molecular $^{18}O_2$ in the gas phase and an atomic ^{16}O of Y_2O_3 can occur above 350 °C.[24] This result is consistent with the earlier observation that lattice oxygen species of Y_2O_3 did not participate directly in the oxidation of methane. The mass 32 signal was notably more intense than in Fig. 2a because it likely corresponds to the $N^{18}O$ fragmentation of the $N^{16}O^{18}O$ produced from the reaction of $N^{16}O$ and pulsed $^{18}O_2$. Additionally, a mass 36 signal was observed due to unreacted $^{18}O_2$. The products with $^{18}O_2$ included $CH_3{}^{18}OCH_3$ (m/z = 47) in addition to those observed with $^{16}O_2$, such as $C^{16}O_2$ and $CH_3{}^{16}OCH_3$. The mass 46 signal was more intense, which could be due to contributions from a CO_2 isotopomer ($C^{16}O^{18}O$) probably formed from oxidation of $CH_3{}^{18}OCH_3$. A mass signal due to $C^{18}O_2$ (m/z = 48) was recorded but had no features. Comparison of the amounts of $CH_3{}^{16}OCH_3$ (0.58 ± 0.05 μmol g^{-1}) and $CH_3{}^{18}OCH_3$ (0.043 ± 0.009 μmol g^{-1}) produced indicates that the prevalent oxygen in this reaction was the ^{16}O, with a corresponding isotope effect of r_{18}/r_{16} = 0.074. Notably, the preferential formation of ^{16}DME and the absence of detectable amount of $C^{18}O_2$ confirm that molecular O_2 is not the direct oxidant in this process, because one would expect only ^{18}DME and $C^{18}O_2$ if it were adsorbed O_2 reacting with the methane.

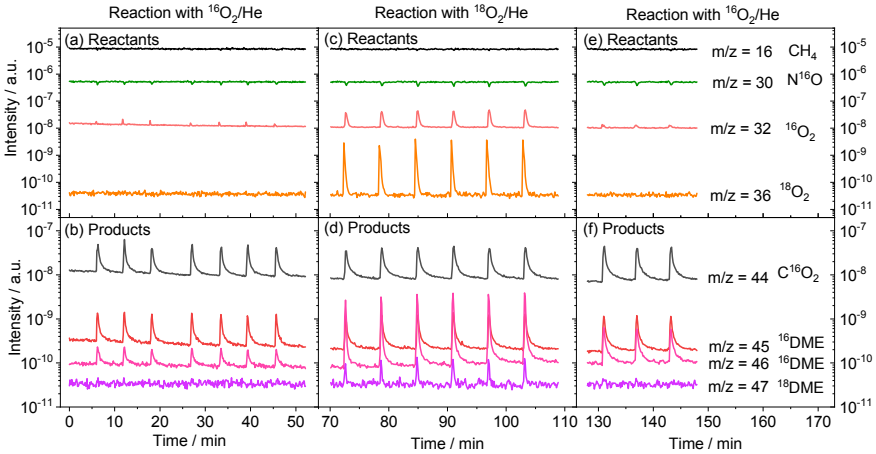

Fig. 2. MS signals versus time for the isotope pulse experiment on a Pt/Y_2O_3 catalyst. Conditions: 100 mg of catalyst with 20% CH_4, 1% NO, 78% He at 325 °C and 0.1 MPa. The results were obtained by injecting 36 μmol pulses of 5% $^{16}O_2$/He (a, b, e, f) or 5% $^{18}O_2$/He (c, d).

Fig. 3 shows a depiction of the likely steps involved in the transformation. The platinum component is responsible for the formation of adsorbed CH_3 species, as is well documented.[25] The yttria support stabilizes a surface nitrate, which transfers an oxygen atom to a CH_3 to form adsorbed OCH_3. Finally, the CH_3 and OCH_3 combine to form DME. The presence of oxygen bound intermediates is key to the selectivity.[26]

The low level of labeled DME compared to unlabeled DME in the $^{18}O_2$ experiment can be understood from the mechanism (Fig. 3) and is due to three factors. First, the dilution of the ^{18}O by half is caused by the use of unlabeled $N^{16}O$; recall that one $^{18}O_2$ reacts with two NO molecules. Second, the further dilution of the ^{18}O by a third occurs because of the reaction of the carrier NO_2 with a surface oxygen atom to form an NO_3 nitrate intermediate; the involvement of NO_3 was evidenced by in situ FTIR measurements.[6] And third, a reduction by the kinetic isotope effect wherein the heavier O reacts at a lower rate than the lighter O for all steps involved in the transfer of oxygen from O_2 to DME. These steps involve a number of consecutive reactions, resulting in a multiplicative effect.

Concerning the first point above, the reaction of $^{18}O_2$ with $N^{16}O$ is more complicated than the stoichiometry of the reaction would suggest as it involves multiple steps as described in the ESI. The transformation proceeds by reaction of O_2 with NO to form planar NO_3 that then reacts with an additional NO to form N_2O_4, which dissociates to form two NO_2. In the course of these reactions the ^{16}O in the two NO and the ^{18}O in O_2 are scrambled to form a 1:1:2 ratio of $N^{16}O_2$, $N^{18}O_2$, $N^{16}O^{18}O$, resulting in dilution of ^{18}O by half. About the second point above, the involvement of a bridging adsorbed nitrate species, NO_3, suggests an additional unlabeled oxygen atom from the yttria support is involved, resulting in a further dilution of ^{18}O by a third; only one of the oxygens in this nitrate is transferred to a methyl group in the formation of a methoxy intermediate. From these relationships, the overall isotope effect will have factors of (1/2) and (1/3) by oxygen dilution, in addition to the series of rate constants from the actual reactions, implying $r_{18}/r_{16} = (1/2)(1/3)\,\Pi_i\left(k_{18}/k_{16}\right)_i$. The last factor is a product of ratios of rate constants for each of the steps *i* in series. For r_{18}/r_{16} = 0.074 obtained in this study, the value of $\Pi_i\left(k_{18}/k_{16}\right)_i$ is 0.44 which for six steps gives an average k_{18}/k_{16} = 0.87. This value is reasonable because a first-order

approximation for k_{18}/k_{16} is the inverse square root of the ratio of the masses[2], which is $\sqrt{M_{16}/M_{18}} = 0.94$. The estimation of the kinetic isotope effect with ^{18}O is rarely done in heterogeneous catalysis because of the closeness in mass to ^{16}O.

The results of the last section (Fig. 2e and f) when $^{16}O_2$ was used after the $^{18}O_2$ exchange measurements are similar to the first section with $^{16}O_2$; the calculated amount of $C^{16}O_2$ is 13 ± 1 μmol g^{-1} and that of $CH_3{}^{16}OCH_3$ is 0.57 ± 0.05 μmol g^{-1}. The formation rates of DME and CO_2 are similar to the initial pulsing, suggesting catalyst stability throughout the experiment.

A final aspect that should be addressed is the possible exchange between $^{18}O_2$ and other species like H_2O and CO_2 present in the system. Work from the literature suggests that this exchange only occurs at very high temperatures (> 700 °C) on SiO_2[27], rare earths[28] and Pt[29].

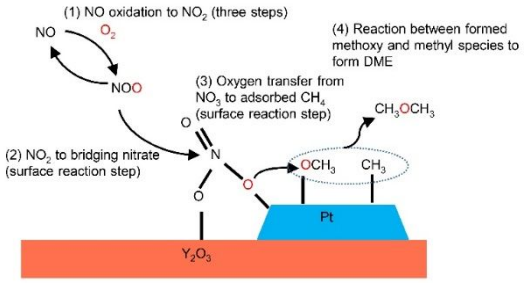

Fig. 3. Schematic of the reaction steps.

Conclusions

Earlier work had shown the unprecedented direct formation of DME from the partial oxidation of methane on a Pt/Y_2O_3 catalyst using an $NO+O_2$ mixture as the oxidant, which occurred through the intermediacy of NO_2 formed in the gas-phase and an adsorbed bridged nitrate NO_3 species. Isotopic labeling in the current study confirms the source of the DME oxygen to be O_2. While NO fed alone resulted in negligible reactivity, pulsing of $^{16}O_2$ or $^{18}O_2$ produced appreciable reactivity. Pulsing with $^{18}O_2$ formed both labeled and unlabeled DME because of isotopic mixing in the formation of NO_2 as well as the NO_3 intermediate. The obtained kinetic isotope effect $k_{18}/k_{16} = 0.87$ is close to the expected value of 0.94. The experiments directly confirm that oxygen from O_2 is the ultimate oxidant because of the formation of quantifiable amounts of labeled DME.

Conflicts of interest

There are no conflicts to declare.

Acknowledgements

This work was supported by the Japan Science and Technology Agency under the CREST program, Grant Number JPMJCR16P2. STO acknowledges Fuzhou University as Mingjiang Chair Professor. We acknowledge Dr. Vibin Vargheese for the catalyst preparation, Dr. So-Jin Ahn for the thermodynamic calculations, and Dr. Yasukazu Kobayashi for discussions.

Notes and references

1. M. Ravi, M. Ranocchiari and J. A. van Bokhoven, *Angew. Chem., Int. Ed. Engl.*, 2017, **56**, 16464-16483.
2. E. V. Kondratenko, T. Peppel, D. Seeburg, V. A. Kondratenko, N. Kalevaru, A. Martin and S. Wohlrab, *Catal. Sci. Technol.*, 2017, **7**, 366-381.
3. M. H. Mahyuddin, Y. Shiota and K. Yoshizawa, *Catal. Sci. Technol.*, 2019, **9**, 1744-1768.
4. A. R. Kulkarni, Z.-J. Zhao, S. Siahrostami, J. K. Nørskov and F. Studt, *Catal. Sci. Technol.*, 2018, **8**, 114-123.
5. K. Yoshizawa, ed., *Direct Hydroxylation of Methane*, Springer, Singapore, 2020.
6. V. Vargheese, J. Murakami, K. K. Bando, I. T. Ghampson, G.-N. Yun, Y. Kobayashi and S. T. Oyama, *J. Catal.*, 2020, **389**, 352-365.
7. J. Xu, R. D. Armstrong, G. Shaw, N. F. Dummer, S. J. Freakley, S. H. Taylor and G. J. Hutchings, *Catal. Today*, 2016, **270**, 93-100.
8. W. Huang, S. Zhang, Y. Tang, Y. Li, L. Nguyen, Y. Li, J. Shan, D. Xiao, R. Gagne, A. I. Frenkel and F. Tao, *Angew. Chem., Int. Ed. Engl.*, 2016, **55**, 13441-13445.
9. Y. K. Chow, N. F. Dummer, J. H. Carter, C. Williams, G. Shaw, D. J. Willock, S. H. Taylor, S. Yacob, R. J. Meyer, M. M. Bhasin and G. J. Hutchings, *Catal. Sci. Technol.*, 2018, **8**, 154-163.
10. M. V. Parfenov, E. V. Starokon, L. V. Pirutko and G. I. Panov, *J. Catal.*, 2014, **318**, 14-21.
11. J. Lu, J. J. Bravo-Suárez, M. Haruta and S. T. Oyama, *Appl. Catal., A*, 2006, **302**, 283-295.
12. F. Bauer, in *Handbook of Heterogeneous Catalysis*, eds. G. Ertl, H. Knözinger, F. Schüth and J. Weitkamp, Wiley-VCH Verlag GmbH& Co. KGaA, Weinheim, Germany, 2008, vol. 1, pp. 1516-1543.
13. S. Knoche, M. Heid, N. Gora, D. Ohlig, J. Steffan, A. Drochner, B. Etzold, B. Albert and H. Vogel, *Catal. Sci. Technol.*, 2020, **10**, 5231-5244.
14. F. Zasada, J. Janas, W. Piskorz, M. Gorczyńska and Z. Sojka, *ACS Catal.*, 2017, **7**, 2853-2867.
15. J. Lao, C. Wan, D.-g. Cheng, F. Chen and X. Zhan, *Catal. Sci. Technol.*, 2020, **10**, 8034-8041.
16. B. Penkala, D. Aubert, H. Kaper, C. Tardivat, K. Conder and W. Paulus, *Catal. Sci. Technol.*, 2015, **5**, 4839-4848.
17. M. Richard, D. Duprez, N. Bion and F. Can, *ChemSusChem*, 2017, **10**, 210-219.
18. G. W. Keulks, *J. Catal.*, 1970, **19**, 232-235.
19. W. Ueda, Y. Moro-oka and T. Ikawa, *J. Catal.*, 1981, **70**, 409-417.
20. L. Urán, J. Gallego, E. Bailón-García, A. Bueno-López and A. Santamaría, *Appl. Catal., A*, 2020, **599**, 117611.
21. V. Vargheese, Y. Kobayashi and S. T. Oyama, *Angew. Chem., Int. Ed. Engl.*, 2020, **59**, 16644-16650.
22. F. C. Meunier, L. Cardenas, H. Kaper, B. Šmíd, M. Vorokhta, R. Grosjean, D. Aubert, K. Dembélé and T. Lunkenbein, *Angewandte Chemie International Edition*, 2021, **60**, 3799-3805.
23. E. Neyrolles, J. Lara Cruz, G. Bassil, F. Contamine, P. Cezac and P. Arpentinier, *Int. J. Chem. Kinet.*, 2020, **52**, 329-340.
24. M. Haneda, M. Tanaka, Y. Doi and N. Bion, *Molecular Catalysis*, 2018, **457**, 74-81.
25. S.-Y. Wu, C.-H. Lin and J.-J. Ho, *Phys. Chem. Chem. Phys.*, 2015, **17**, 26191-26197.
26. S. T. Oyama, *J. Catal.*, 1991, **128**, 210-217.
27. M. Noriyoshi and T. Toshizo, *Bull. Chem. Soc. Jpn.*, 1938, **13**, 601-607.
28. P. Lakshmanan, F. Averseng, N. Bion, L. Delannoy, J.-M. Tatibouët and C. Louis, *Gold Bull.*, 2013, **46**, 233-242.

29. Y. L. Sandler and D. D. Durigon, *J. Phys. Chem.*, 1968, **72**, 1051-1057.